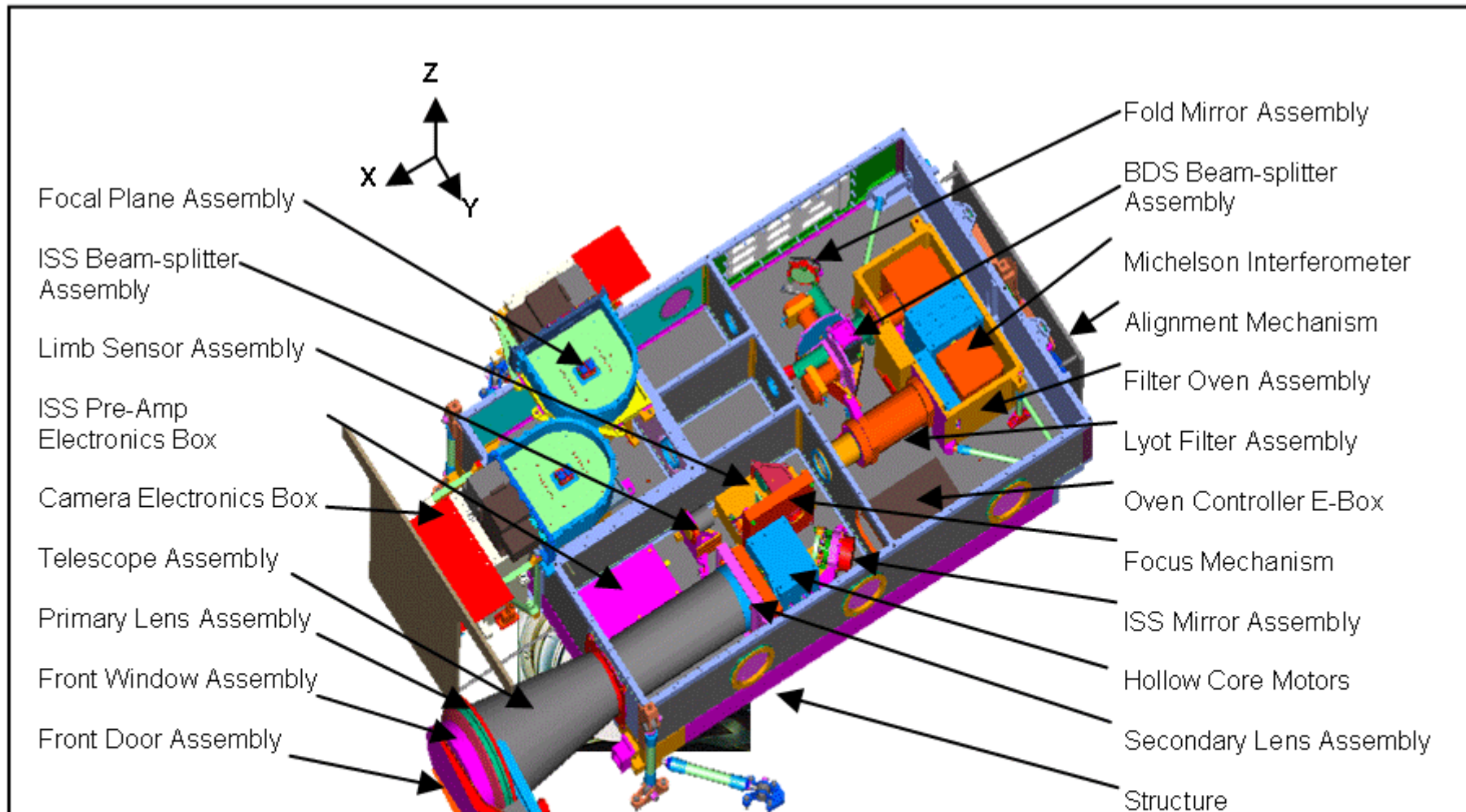


4+ YEARS OF SCIENTIFIC RESULTS WITH SDO/HMI

Sebastien Couvidat and the HMI team

Solar Metrology Symposium, October 2014

The HMI Instrument



Optical Characteristics:

Effective Focal Length: 495 cm
 Telescope Clear Aperture: 14 cm
 Focal Ratio: $f/35.4$
 Final Image Scale: $24 \mu\text{m} / \text{arcsec}$
 Re-imaging Lens Magnification: 2
 Focus Adjustment Range: 16 steps of 1 mm

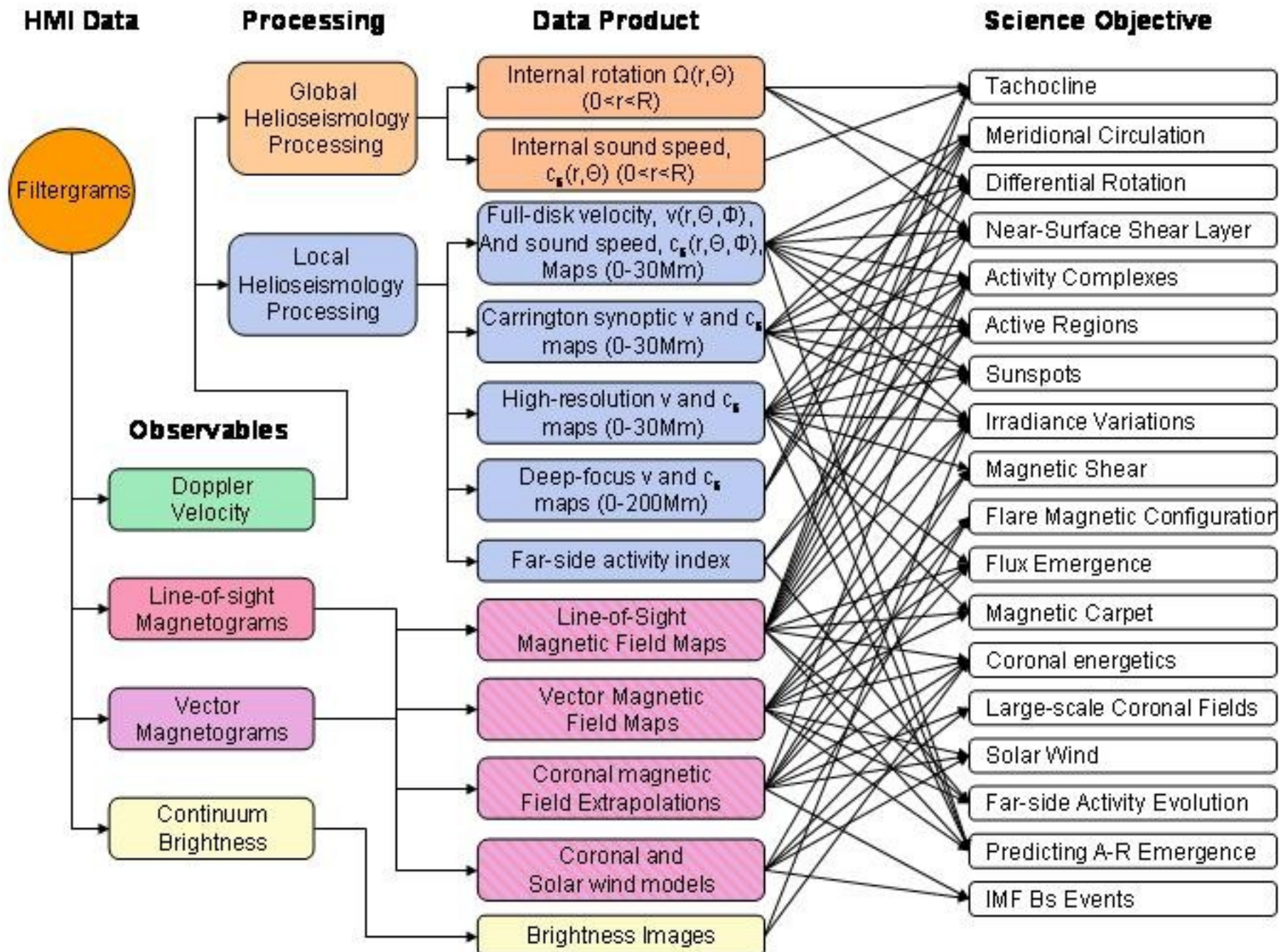
Filter Characteristics:

Central Wavelength: 617.3 nm
 Reject 99% Solar Heat Load
 Bandwidth: 0.0076 nm
 Tunable Range: 0.05 nm
 Free Spectral Range: 0.0688 nm

Mechanical Characteristics:

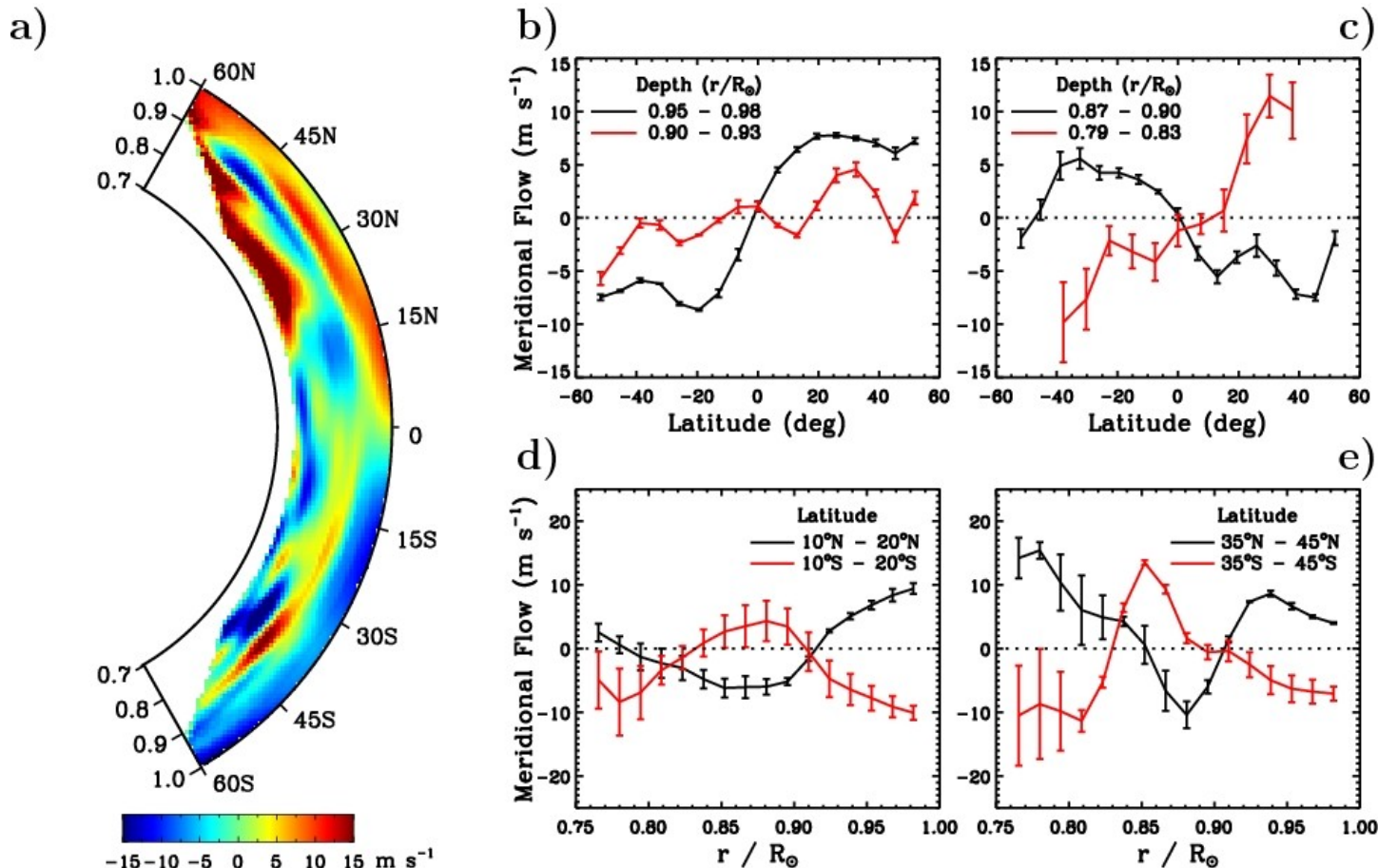
Box: $0.84 \times 0.55 \times 0.16 \text{ m}$
 Over All: $1.19 \times 0.83 \times 0.30 \text{ m}$
 Mass: 42.15 kg
 First Mode: 73 Hz

HMI Science Goals



Evidence of Double-Cell Meridional Circulation inside the Sun

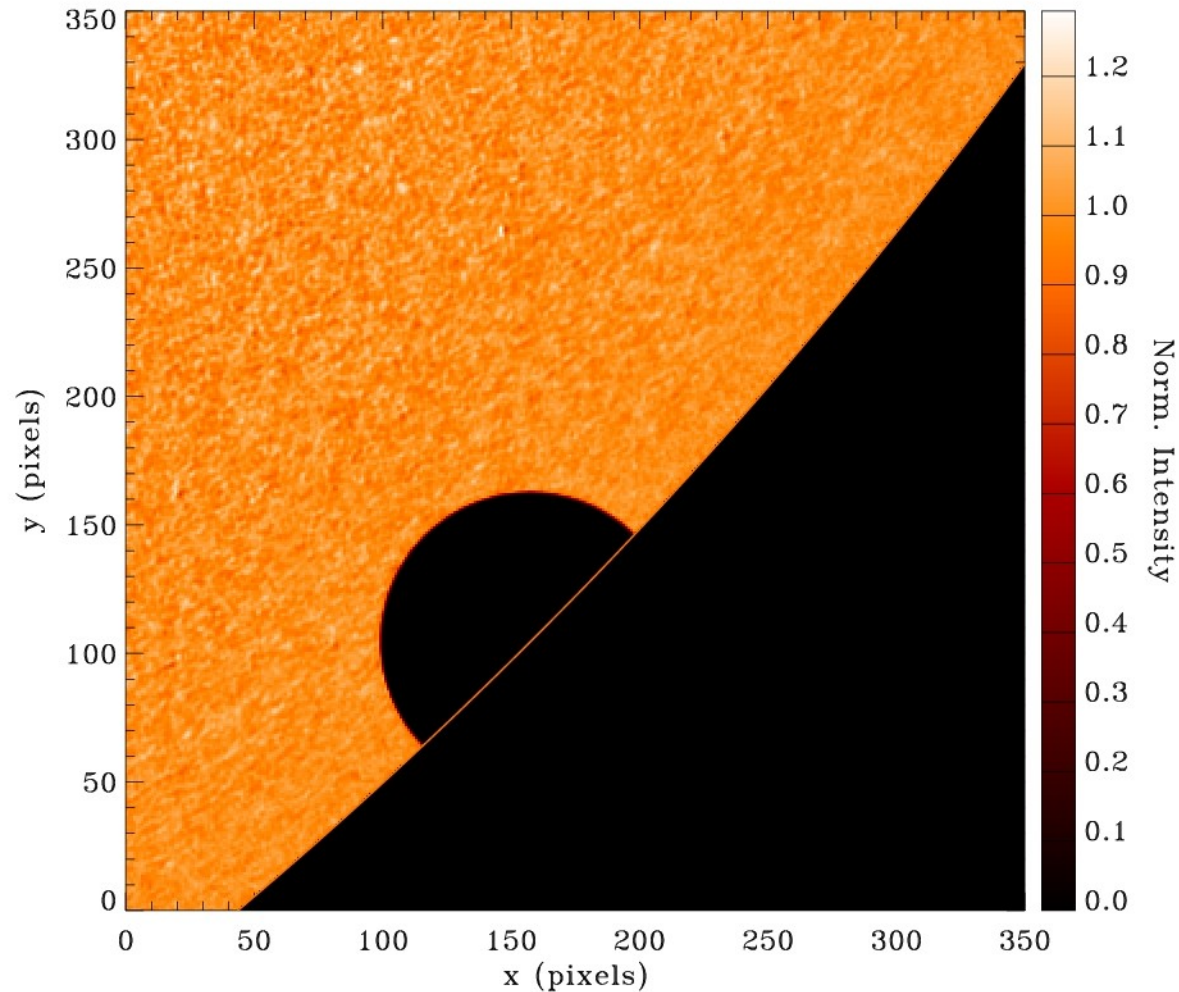
From: Zhao, J., Bogart, R. S., Kosovichev, A. G., Duvall, T. L., Jr., Hartlep, T. 2013, ApJL, 774, L29



Meridional flow profile, obtained by inverting the measured acoustic travel times. Panel (a) shows a cross-section view of the meridional-flow profile, with the positive velocity directing northward. Panels (b) and (c) show the inverted velocity as functions of latitude averaged over several depth intervals. Panels (d) and (e) show the velocity as functions of depth averaged over different latitudinal bands.

Measuring the Solar Radius with the Venus Transit

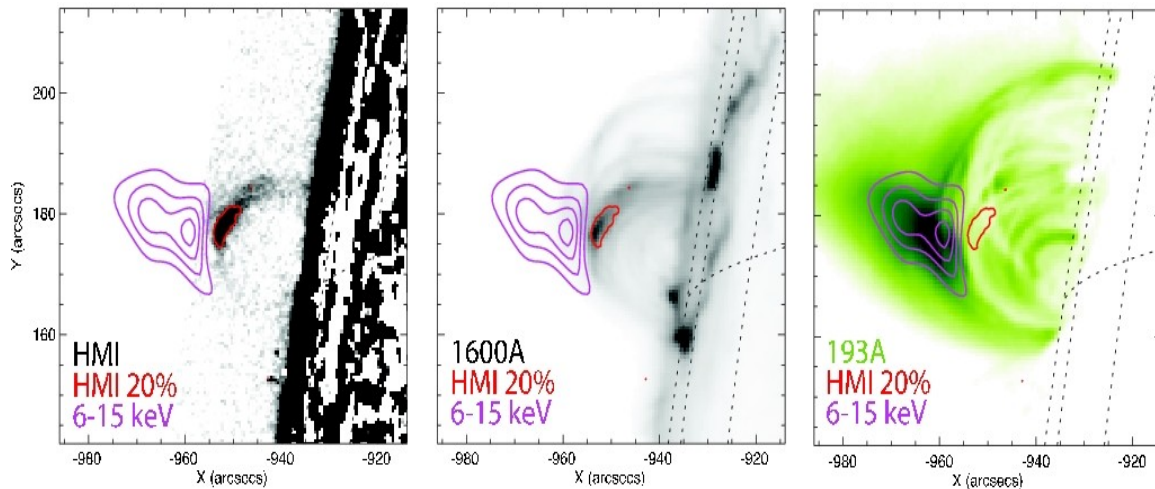
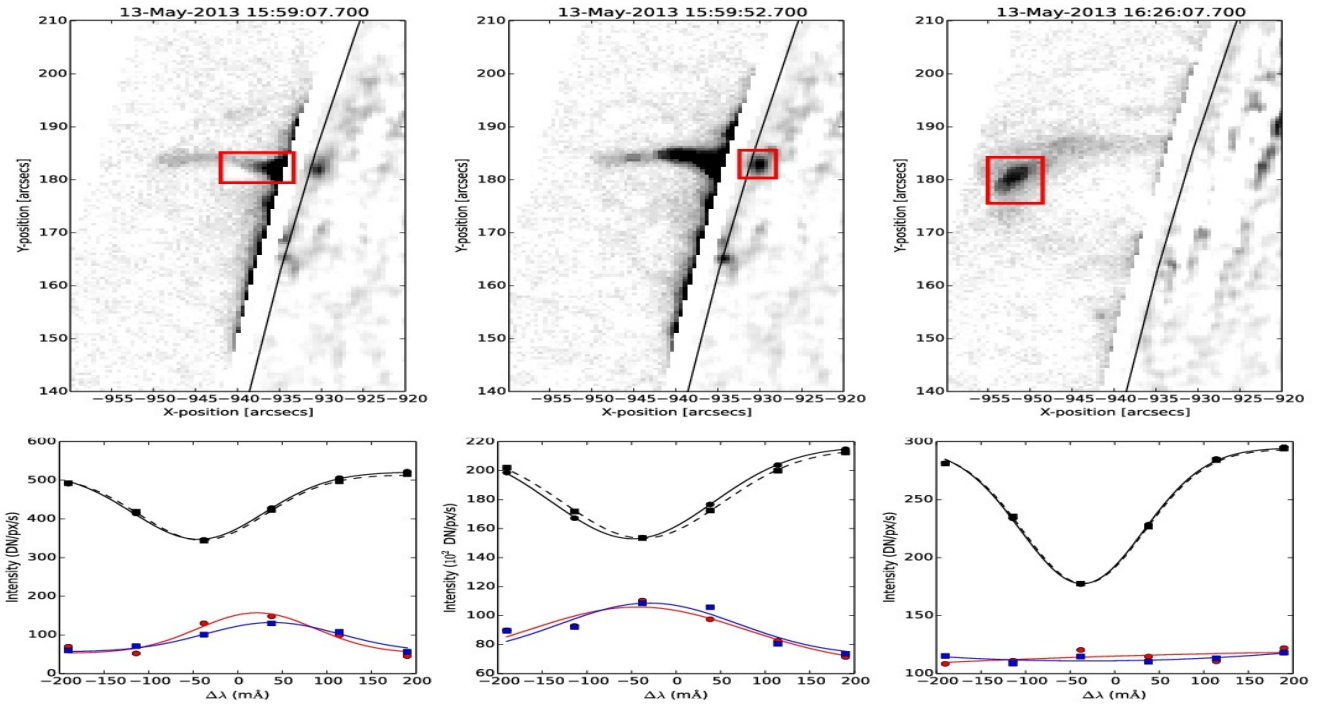
From: Emilio, M., Couvidat, S., Bush, R.I, Kuhn, J.R., and Scholl, I.F., accepted for publication in ApJ



Best estimated radius (using inflection point of limb-darkening function as definition): $959.57'' \pm 0.02''$

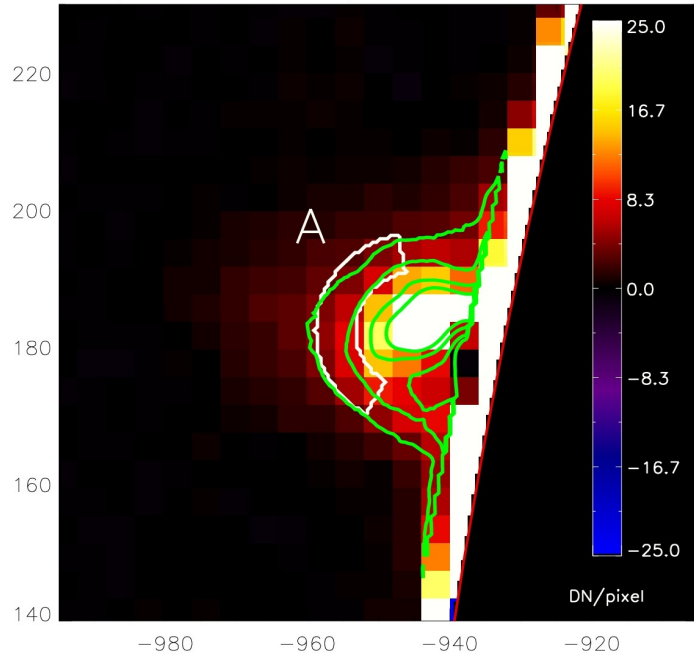
HMI as a Coronagraph

From: Martinez Oliveros, J.C., Couvidat, S., Schou, J., Krucker, S., Lindsey, C., Hudson, H.S, and Scherrer, P., Solar Physics, 2011, 269

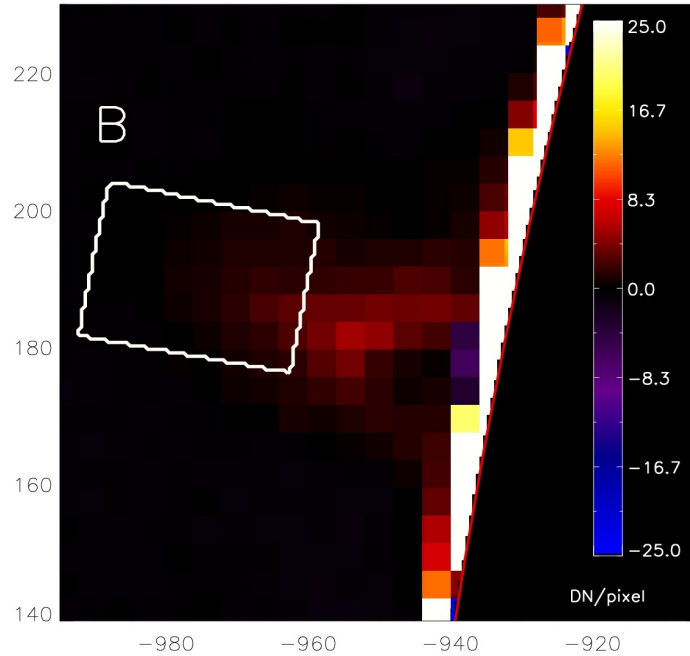


Observation of Linear Polarization in a Prominence and Flare

HMI/Stokes I 13-May-2013 16:16:41.097 UT



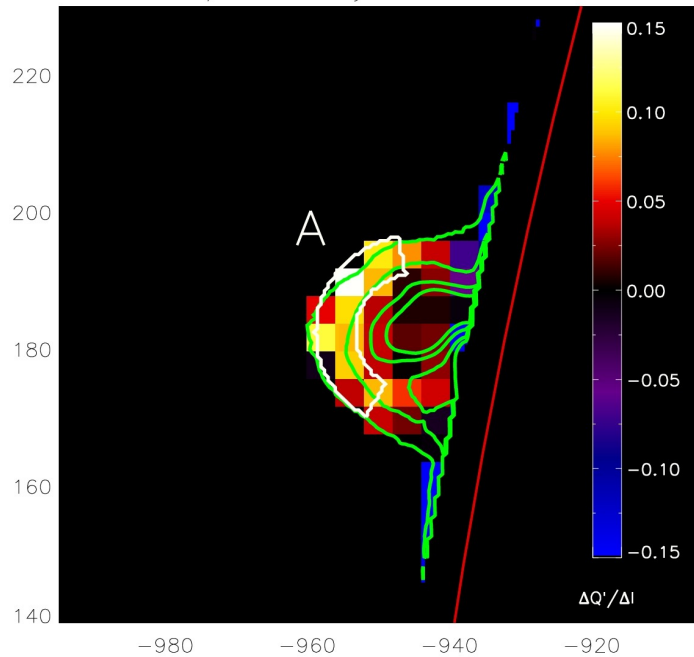
HMI/Stokes I 13-May-2013 17:12:56.097 UT



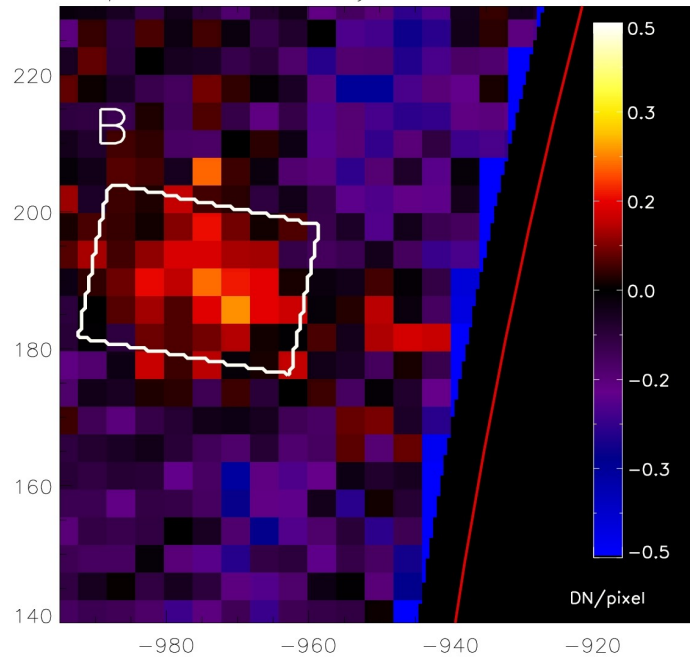
From: Saint-Hilaire, P., Schou, J., Martinez Oliveros, J.C., et al., ApJ, 2014, 786L

Linear polarization is produced by Thomson scattering

Stokes $\Delta Q'/\Delta I$ 13-May-2013 16:16:41.097 UT

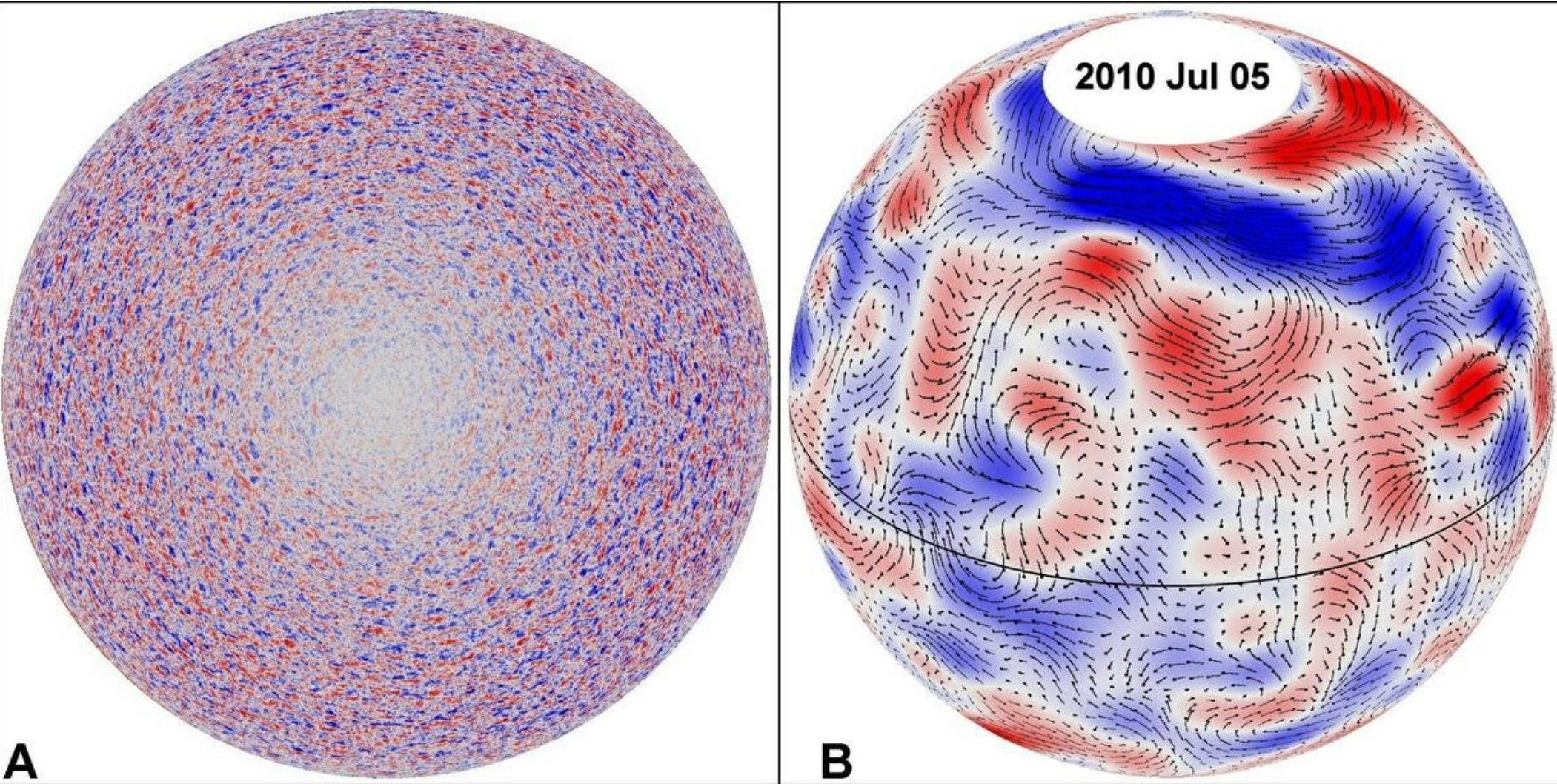


HMI/Stokes Q' 13-May-2013 17:12:56.097 UT



Giant Cells

From: Hathaway, D.H., Upton, L., and Colegrove, O., Science, 2013, 1217



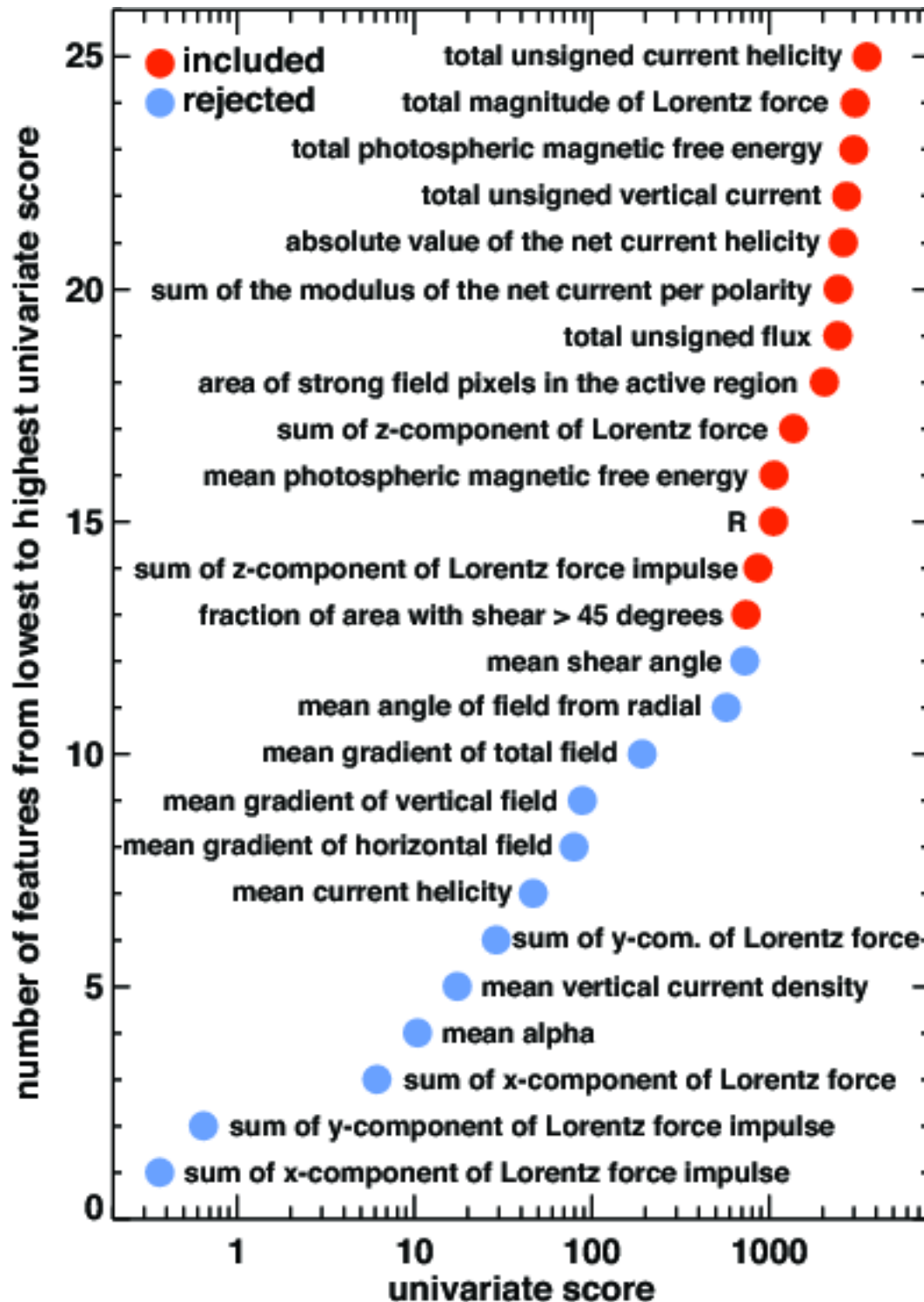
Evidence of long-lasting (several months) cells as large as 500 Mm, that transport angular momentum from the poles to the equator and maintain the solar differential rotation

Solar Flare Forecasting

From: Bobra, M. and Couvidat, S.
submitted to ApJ

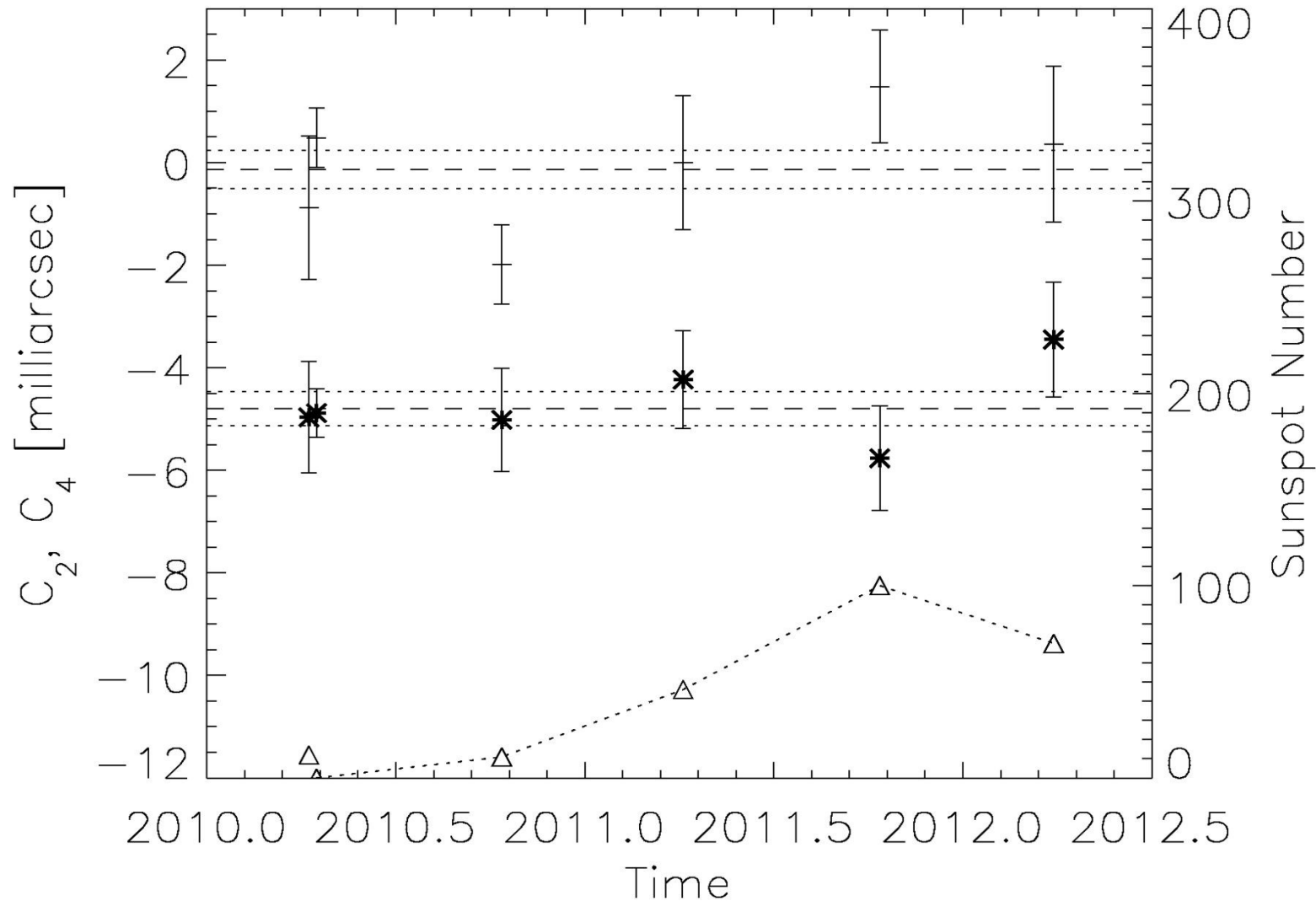
Using 25 SHARP parameters
characterizing active regions

We also used feature selection to
determine which photospheric
characteristics of an active region are
best predictor of its flare productivity
(for M- and X-class flares)



The Precise Solar Shape and Its Variability

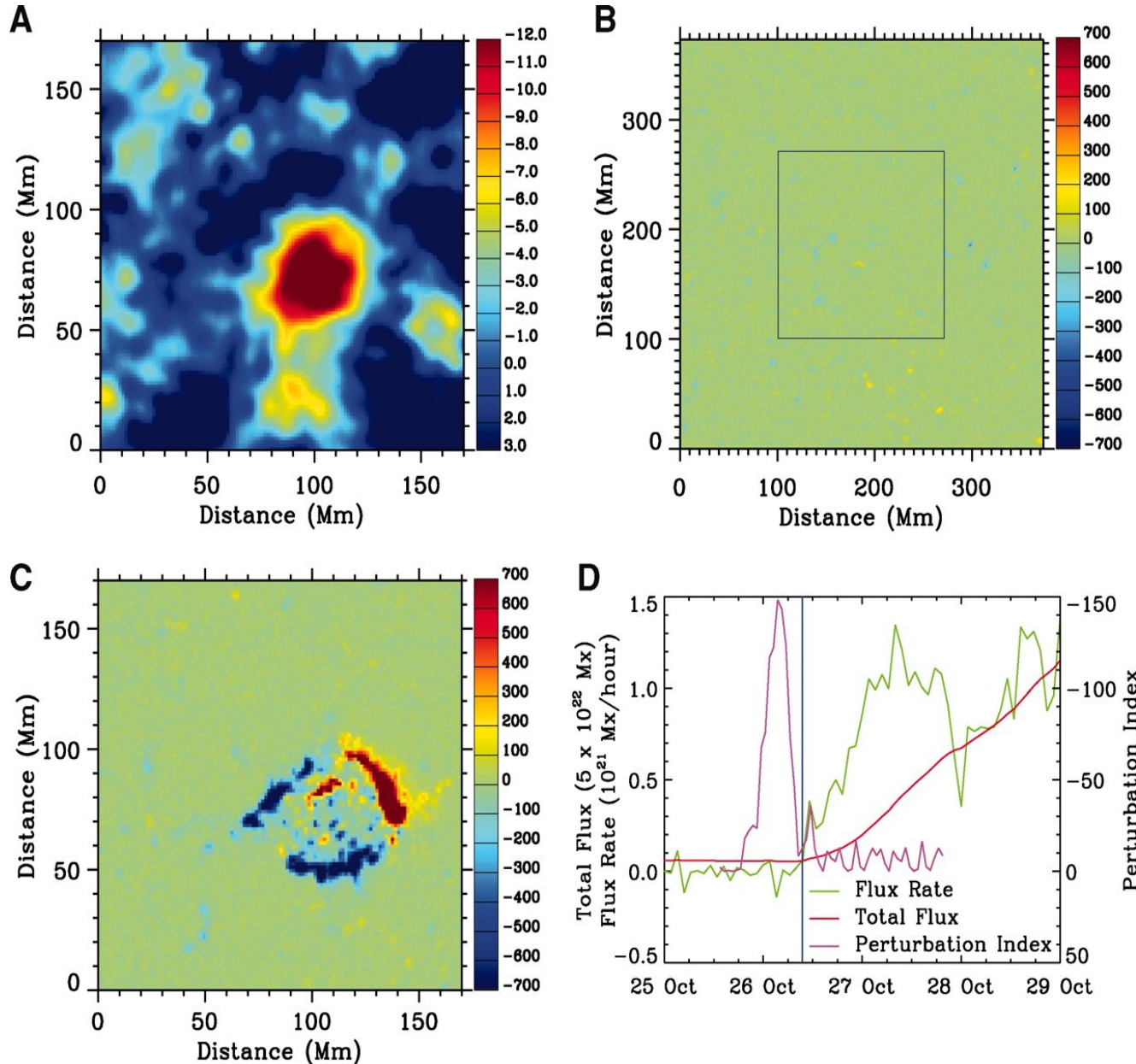
From: Kuhn, J.R., Bush, R., Emilio, M., and Scholl, I.F., Science, 2012, 337, 1638



The oblateness (star) and hexadecapole (dash) coefficients for 6 HMI rolls. Triangles show the 3 days averaged sunspot number. The horizontal lines show the means and standard deviations.

EMERGING FLUX IN CONVECTION ZONE

From: Ilonidis, S., Zhao, J., and Kosovichev, A.G., Science, 2011, 333, 993

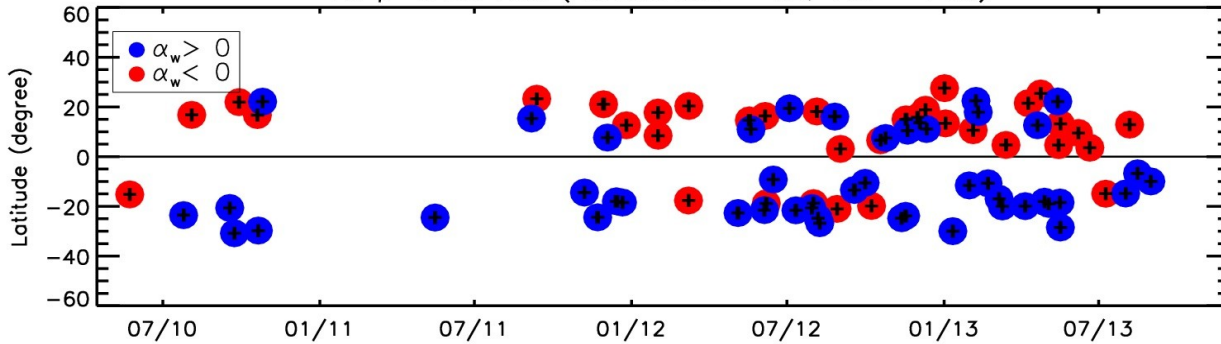


(A) Mean travel-time perturbation map (in seconds) of AR 10488 at a depth of 42 to 75 Mm, obtained from an 8-hour data set 28.5 h prior to peak flux. (B) Photospheric magnetic field (in gauss) at the same time as (A). The whole map corresponds to the region where the computations were carried out, whereas the squared area at the center corresponds to the region shown in (A). (C) Photospheric magnetic field (in gauss) at the same location as (A) but 24 hours later. (D) Total unsigned magnetic flux (red line) and magnetic flux rate (green line) of AR 10488. The vertical blue line marks the start of emergence. The pink line shows the temporal evolution of the perturbation index (in units of 125 s Mm^2), which is defined as the sum of travel-time perturbations with values lower than -5.4 s , within the signature of (A).

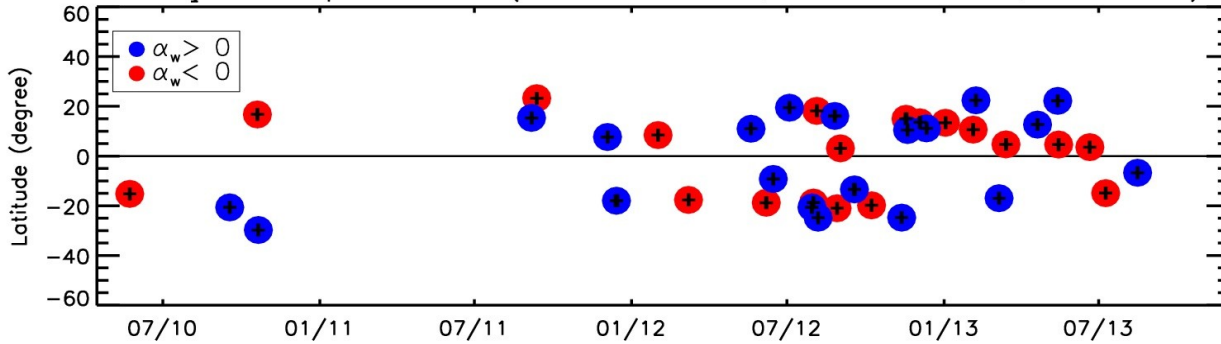
Testing Hemispheric Rule of Helicity

From: Liu, Y., Hoeksema, J.T. and Sun, X., ApJ, 2014, 783, 1L

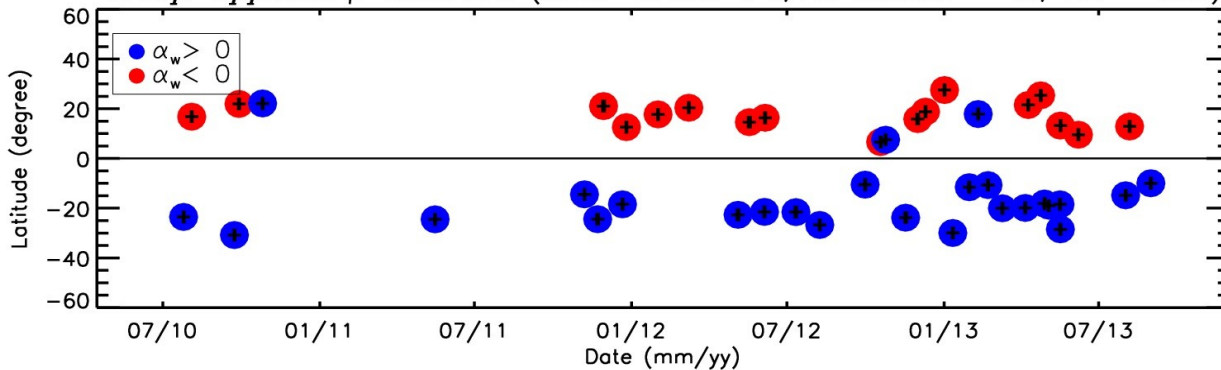
All β -class ARs (AR Number = 82; Yes = 76%)



Group-Same β -class ARs (Twist \cdot Writhe > 0 ; AR Number = 39; Yes = 56%)



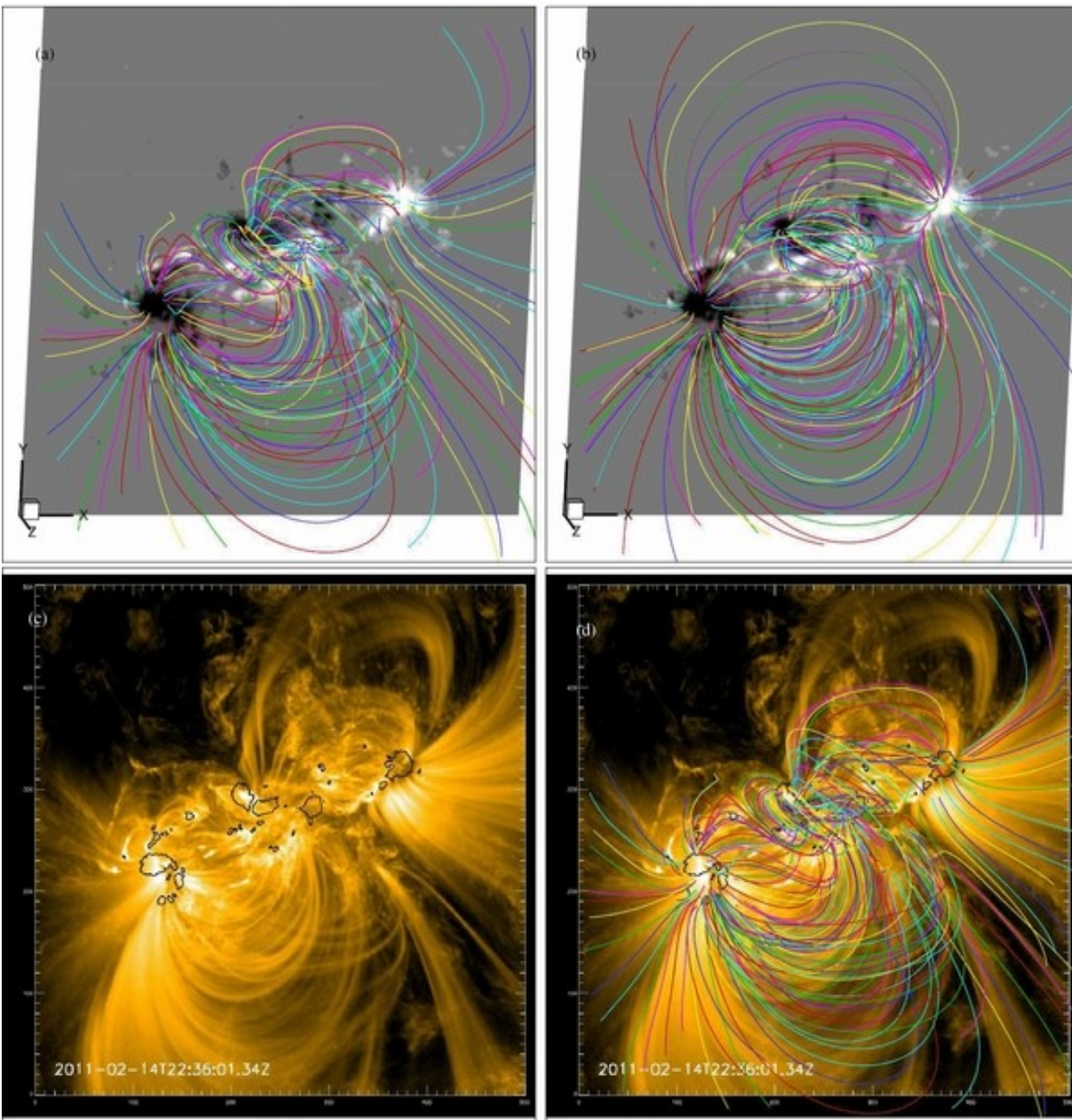
Group-Opposite β -class ARs (Twist \cdot Writhe < 0 ; AR Number = 43; Yes = 93%)



Distribution of sign of twist in bipolar ARs as a function of latitude and time for Solar Cycle 24 from May 2010 to November 2013. The titles of the plots indicate the sample size ("AR Number") and the degree of hemispheric preference ("Yes") that refers to percentage of the ARs in the sample obeying the hemisphere rule. Top panel is for all ARs; middle is for ARs having the same signs of twist and writhe; bottom is for ARs having the opposite signs of twist and writhe.

EXTRAPOLATION OF CORONAL FIELD

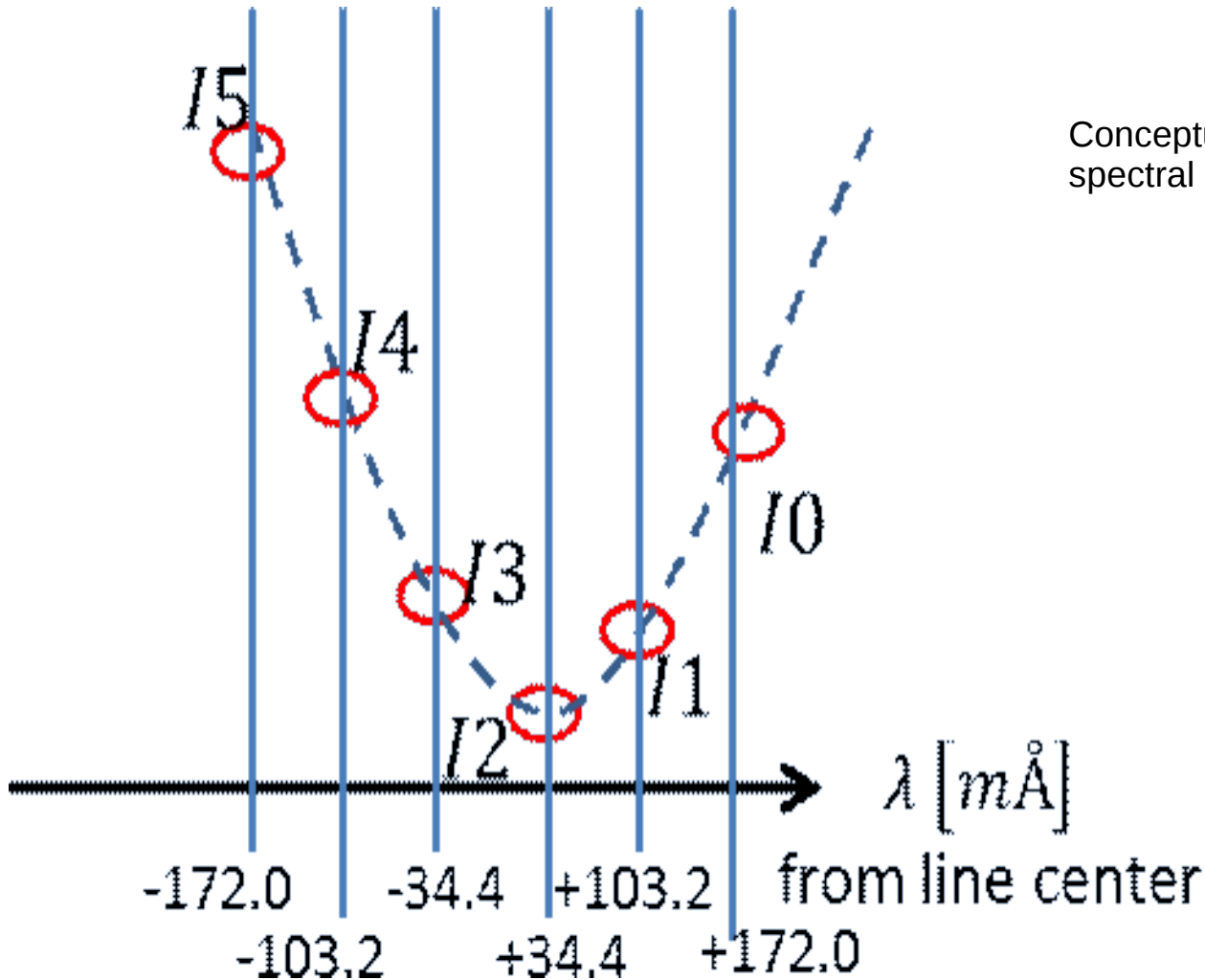
From: Jiang, C. and Feng, X., ApJ, 2013, 769, 144



Comparison of extrapolation field lines with AIA 171 Å loops for AR 11158: the NLFFF lines (a), the potential field lines (b), the AIA image (c) and NLFFF lines overlaying the AIA image (d). Contour lines for ± 1000 G (the black curves) of line-of-sight photospheric field are overplotted on the AIA images, and for all the panels the field lines are traced from the same set of footpoints on the bottom surface.

SDO/HMI Multi-height Dopplergrams

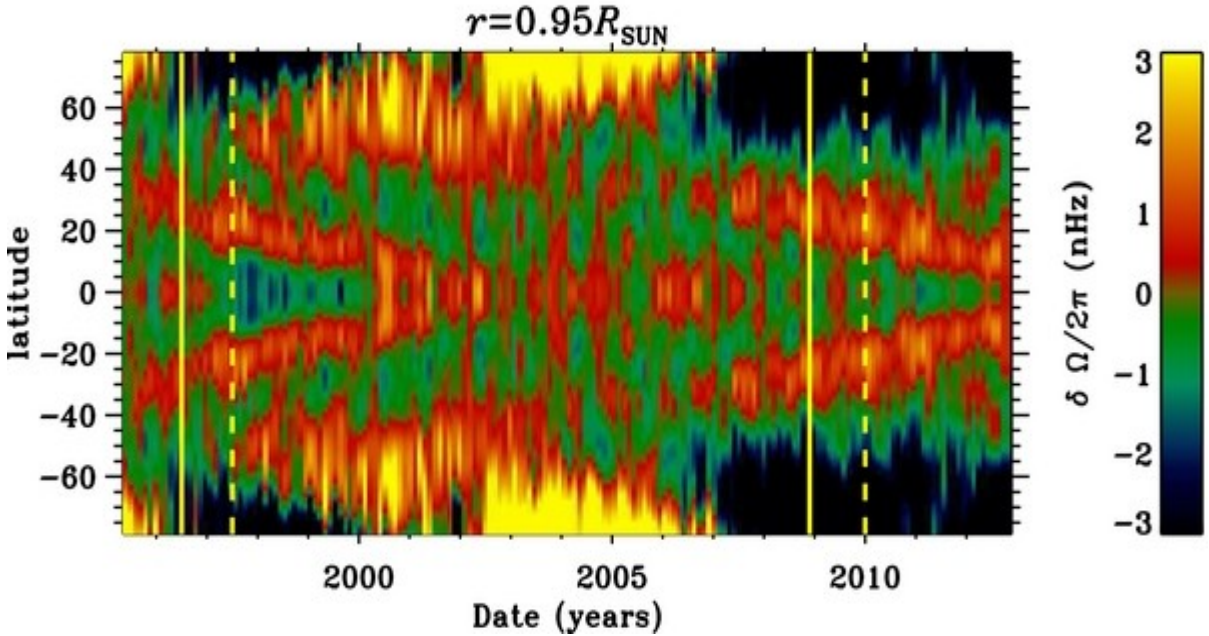
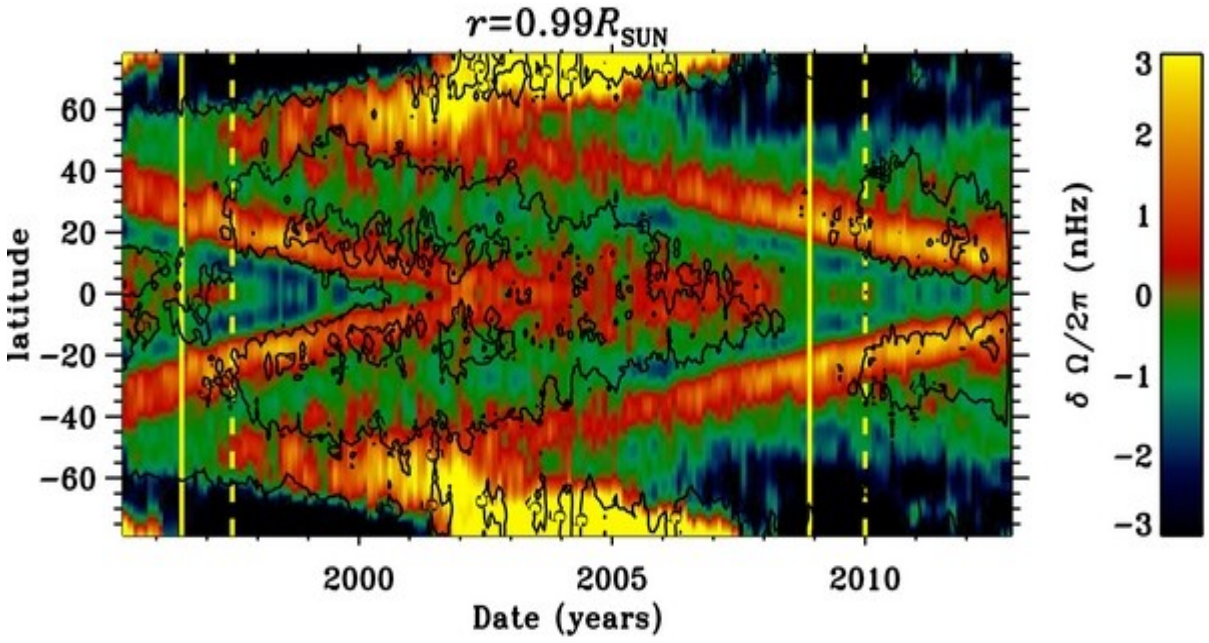
From: Nagashima, K., Löptien, B., Gizon, L., Birch, A. C., Cameron, R., Couvidat, S., Danilovic, S., Fleck B., and Stein, R., Solar Physics, 2014, 289, 3457



Conceptual illustration of the Fe I 617.3 nm spectral line and HMI filter positions.

SOLAR TORSIONAL OSCILLATIONS IN THE RISING PHASE OF CYCLE 24

From: Howe, R., Christensen-Dalsgaard, J., Hill, F., Komm, R., Larson, T.P., Rempel, M., Schou, J., and Thompson, M.J., ApJ, 2013, 767, 20L



Combined rotation-rate residuals from GONG, MDI, and HMI 2dRLS inversions at selected depths. The solid yellow vertical lines mark the solar minima and the dashed yellow lines the onset of widespread activity at the start of the new cycle. The top panel also shows the 5, 25, and 45 G contours of unsigned magnetic field strength from Kitt Peak magnetograms.

Conclusion

In this brief review I wanted to emphasize the breadth and scope of scientific research performed with HMI data

A lot of exciting and valuable results have been obtained with HMI since the launch of SDO in February 2010

More than 700 articles/conference proceedings using HMI data according to NASA ADS

We hope the mission will be extended next year

The website hmi.stanford.edu/hminuggets provides the latest scientific discoveries made with HMI data